INT. J. REMOTE SENSING, 2002, VOL. 23, NO. 6, 1043–1062

Taylor & Francis
Taylor & Francis Group

# Mapping of several soil properties using DAIS-7915 hyperspectral scanner data—a case study over clayey soils in Israel

E. BEN-DOR[1], K. PATKIN[1], A. BANIN[2] and A. KARNIELI[3]

[1]Department of Geography, Tel-Aviv University, Ramat Aviv, Tel-Aviv
[2]Department of Soil and Water Sciences, Faculty of Agricultural, Food and Environmental Quality Sciences, The Hebrew University, Rehovot, Israel
[3]J. Blaustein Institute for Desert Research Sde-Boker Campus, Negev, Israel

(*Received 28 September 1999; in final form 5 June 2000*)

**Abstract.** The data acquired from the hyperspectral airborne sensor DAIS-7915 over Izrael Valley in northern Israel was processed to yield quantitative soil properties maps of organic matter, soil field moisture, soil saturated moisture, and soil salinity. The method adopted for this purpose was the Visible and Near Infrared Analysis (VNIRA) approach, which yields an empirical model for predicting the soil property in question from both wet chemistry and spectral information of a representative set of samples (calibration set). Based on spectral laboratory data that show a significant capability to predict the above soil properties and populations using the VNIRA strategy, the next step was to examine this feasibility under a hyperspectral remote sensing (HSR) domain. After atmospherically rectifying the DAIS-7915 data and omitting noisy bands, the VNIRA routine was performed to yield a prediction equation model for each property, using the reflectance image data. Applying this equation on a pixel-by-pixel basis revealed images that described spatially and quantitatively the surface distribution of each property. The VNIRA results were validated successfully from a priori knowledge of the area characteristics and from data collected from several sampling points. Following these examinations, a procedure was developed in order to create a soil property map of the entire area, including soils under vegetated areas. This procedure employed a random selection of more than 80 points along nonvegetated areas from the quantitative soil property images and interpolation of the points to yield an isocontour map for each property. It is concluded that the VNIRA method is a promising strategy for quantitative soil surface mapping, furthermore, the method could even be improved if a better quality of HSR data were used.

## 1. Introduction

Hyperspectral remote sensing (HSR) is an advanced technique that provides a near-laboratory-quality reflectance spectra of each single pixel. This capability allows the identification of targets based on their well-known spectral absorption features (Goetz *et al.* 1985). Under laboratory conditions, the spectral information of the visible, near-infrared and short wave infrared (VIS-NIR-SWIR; 0.4–2.5 $\mu$m) spectral regions provides a promising capability to identify soil, vegetation, rock and mineral materials (e.g. Stoner and Baumgardner 1981, Gao and Goetz 1990, Clark *et al.* 1990). Under HSR conditions, this spectral information enables semi-quantitative

*International Journal of Remote Sensing*
ISSN 0143-1161 print/ISSN 1366-5901 online © 2002 Taylor & Francis Ltd
http://www.tandf.co.uk/journals
DOI: 10.1080/01431160010006962

classification of large areas regarding such issues as composition of rocks and minerals (Kruse *et al.* 1990, Lorcher 1999, Hausknecht 1999, vegetation status (Martin and Aber, 1993, Gao and Goetz 1995), water body condition (Keller *et al.* 1998, Lazar *et al.* 1998, Pierson 1998) and atmospheric gas distribution (Gao and Goetz 1990, Richter and Ludeker 1998).

Because soil is a complex system, soil properties cannot be easily assessed directly from their reflectance spectra even under controlled (laboratory) conditions (Ben-Dor and Banin 1994). Since under a remote sensing domain this capability could be even more problematic (Peng 1998), neither quantitative nor semi-quantitative spatial analysis of many soil properties from reflectance data have yet received proper attention in either the point or imaging spectroscopy domain. Nevertheless, in some cases, quantitative feasibility can be achieved using HSR data, mainly if the property in question is a well-known spectral property active across the reflectance region (e.g. organic matter, Ubelhoven *et al.* 1997).

A new approach for analysing soil properties from laboratory reflectance information has been developed by Dalal and Henry (1986) and later expanded by Ben-Dor and Banin (1995a, 1995b). The method (termed VNIRA; Visible and Near Infrared Analysis) was originally developed for use in food science for rapidly determining chemical constituents directly from their laboratory reflectance spectra in the NIR-SWIR spectral region (1.0–2.5 $\mu$m) (Norris 1988). This approach employs a statistical model that draws a correspondence between 'wet chemistry' and reflectance data to yield a tool for empirically predicting the constituent in question solely from its reflectance information. The VNIRA method is widely used in fields such as food science, tobacco and oil industries, pharmacology, vegetation monitoring and medicine (Stark *et al.* 1986). In the field of remote sensing, extracting reflectance values from a pixel is a complicated task as compared with the process under controlled laboratory conditions, because of illumination and terrain changes, atmospheric attenuation, low signal-to-noise ratio and more. However, if the airborne sensor is sensitive enough and the atmospheric effects can be properly removed from the original data, this technique might be useful for rapid quantitative mapping of large areas. In this regard Curan *et al.* (1992) and LaCapra *et al.* (1996) were able to demonstrate that the VNIRA approach is capable of assessing canopy chemistry by using AVIRIS (Airborne Visible and Infrared Imaging Scanner; Vane *et al.* 1993) HSR data. Soil is a more heterogeneous material than vegetation, which eventually results in greater difficulties in applying quantitative analyses to HSR soil data. Ben-Dor and Banin (1990, 1994, 1995a, 1995b) have shown that the VNIRA approach is useful for assessing soil properties if careful laboratory conditions and spectral manipulation techniques are employed. Moreover, they showed that for several soil properties, a large number of spectral channels is not always required to accurately predict the property in question (number of channels required ranged between 15 and 313). Because airborne HSR technology enables band numbers around this range (e.g. AVIRIS-224, DAIS-79), the VNIRA approach should be examined for soil applications using HSR data. To the best of our knowledge, this approach has never been applied to a soil environment in a remote sensing domain. This study is therefore aimed at examining the HSR-VNIRA capability under such conditions.

## 2. Materials and methods

### 2.1. *The selected sensor and area*

The DAIS-7915 scanner was selected for this study. The DAIS-7915 is a whisk broom sensor, manufactured by the GER Inc., USA and upgraded by the DLR

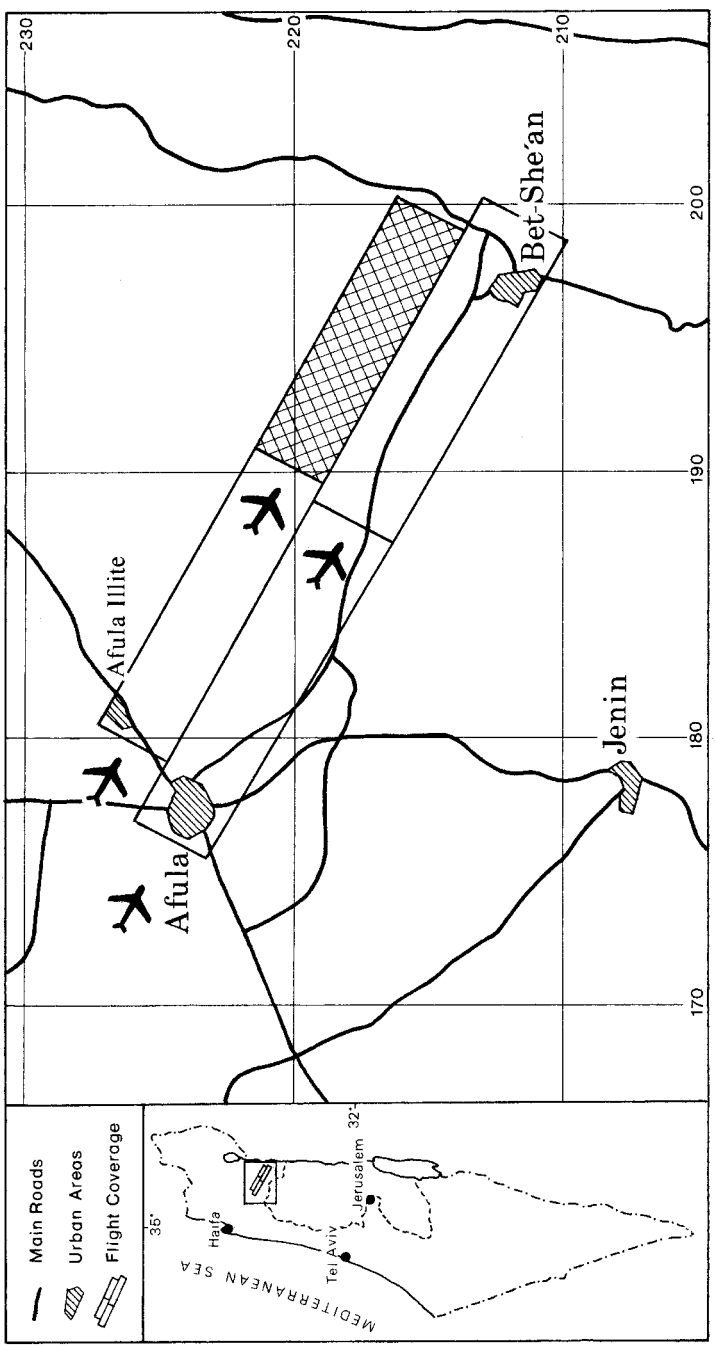


Figure 1. Location of the study area. From the four flight overpasses acquired in this DAIS mission, the shaded polygon represents the study area of Zvaim Heights. (The small map is provided in a geographical coordination system for global positioning, where the major map is provided in the internal old Israel coordination system for local positioning).

Germany (Muller and Ortel 1997). The sensor is sensitive to the VIS-NIR-SWIR-TIR spectral regions (0.4–14 $\mu$m), consisting of 79 channels across, with a bandwidth ranging from 0.9 nm to 60 nm. The instantaneous-field-of-view (IFOV) is 3.3 mrad, and the field-of view (FOV) is 52°. For this study only the refractive portion of the electromagnetic radiation was taken covering the VIS-NIR-SWIR (0.4–2.5 $\mu$m) spectral region with 72 spectral bands. The sensor was mounted onboard a DLR Dornier 228 aircraft and flown over several Israel locations during the summer of 1997 from an altitude of 10 000 feet (providing a pixel size of about 8 m $\times$ 8 m). The area selected for this study is in northern Israel (Izrael Valley) on a relatively flat terrain called Zvaim Heights (figure 1). This area is heavily cultivated and intensively used to grow agricultural crops. The soil texture is heavy clay (mostly vertisol in the USDA classification system), which causes many related problems, such as poor drainage, salinity and heavy structure.

### 2.2. *Data acquisition*

The overflight took place on 2 August, 1997, at 15:00 local time (12:00 GMT). On the ground, several teams measured field spectra, using a field portable spectrometer (Analytical Spectral Devices—ASD), and surface temperature, using a thermal radiometer gun. Also, 62 soil samples were collected from throughout the area during the overpass. The soil sampling was carefully done as follows: for each soil sample, a uniform area measuring about four pixels ($\sim$30 m $\times$ 30 m) was selected. Each target area was described in detail in the field, accurately georeferenced, using a GPS device, and photographically documented. Four to five samples from the upper layer of the selected 30 m $\times$ 30 m area were mixed to yield a representative soil composite for further analysis. The selection of sample areas was based on minimal variation between airborne and field spectra, which was visually detected during the sampling time. The soil samples were stored in plastic bags in order to preserve the in-field soil moisture and were brought into the laboratory for chemical and physical analyses.

### 2.3. *Wet chemistry analyses*

The soil field moisture was determined by the oven drying method after Gardner (1986) (weighing the samples before and after 24 hours in a 105°C environment). The organic matter content was determined by using the loss-on-ignition method after Ben-Dor and Banin (1989) (heating the sample to 400°C for 8 hours and calculating the weight (organic) loss on a dry soil basis). The soil was brought to the saturated moisture condition using distilled water. After equilibration for 60 minutes, the soil solution was extracted using a vacuum of $\sim$0.3 atmospheres. The extracted solutions were stored in glass bottles under refrigeration for further analysis. The electrical conductivity (EC) at 25°C and the pH of the extracted solutions were analysed. The saturated moisture content was determined using the oven drying method (see above). In addition to all of the above measurements, the soils were identified by colour using a Munsell colour chart and measured for their reflectance under laboratory conditions using two spectrometers (ASD with 2100 channels across the 0.4–2.5 $\mu$m spectral region and LT-1200 with 1200 channels across the 1.2–2.4 $\mu$m spectral region). A comparison between field and laboratory spectra revealed a good match at the known atmospheric windows, whereas better signal-to-noise ratios were observed in the laboratory spectra recorded by the LT-1200 spectrometer at around 2.1–2.4 $\mu$m).

2.4. *DAIS-7915 data processing*

The DAIS data were converted into radiance data using a calibration file provided by the DLR (based on a laboratory calibration performed by the Optoelectronics Laboratory of the DLR before the flight). Whereas most of the DAIS channels visually provided sharp images, apparently channels 60–70 (between 2.314 and 2.462 $\mu$m) were contaminated with nonsystematic across-track noise. Using the Minimum Noise Fraction (MNF) technique (Green *et al.* 1988), the noise components were isolated from the spectral components and the data spectral cube was reconstructed to yield clean images of channels 60–67. Using this method, the noise from channels 68–70 could not be removed and therefore they were omitted from the entire reconstructed image cube.

Atmospheric effects were removed by applying several methods and models on the radiance data as follows: ATREM (Gao *et al.* 1993), ATCOR (Richter 1996), MODTRAN (Berk *et al.* 1989), flat field; IARR (Kruse 1988) and Empirical Line (EL; Roberts *et al.* 1985) techniques. The best method for providing the most reliable results (as examined against field soil spectra) was the EL technique with seven targets. Accordingly, the radiance data (MNF treated) were corrected for further analysis using this selected EL technique. Nevertheless, because spectral noise across the 2.2–2.5 $\mu$m wavelengths (channels 62–67) were still visible after the atmosphere rectification, this range was gently smoothed by using a moving average reduction technique.

Locating each soil sample on the image was possible using Differential Global Position System (DGPS) information recorded during the data acquisition (both in the air and on the ground) and by using the detailed information collected for each of the targets during the time of acquisition. DAIS reflectance spectra (resulting from the EL correction) of each sample (generated from 5–10 pixels around a well-defined location of each target as obtained either by using the DGPS information or relying on the detail field description of each selected area) were extracted and transferred to a new environment in order to perform the VNIRA procedure independently.

2.5. *Spectral analyses*

The reflectance $R$ (or its first derivatives $R'$; $R' = (R_\lambda - R_{\lambda-1})/\Delta\lambda$, where $R$ is the reflectance at wavelength $\lambda$ and $\Delta\lambda$ is the spectral interval between two closed spectral bands ($\lambda$ and $\lambda - 1$)) of each wavelength for all samples (laboratory and atmospherically corrected airborne data) were linearly correlated against the analysed value of the given chemical property. A correlogram spectrum for each property, showing the coefficient of regression versus the wavelengths, was performed. The next step was to select the highest (in terms of coefficient of correlation) and most reliable 38 bands and their corresponding readings (field, laboratory and airborne) to run a forward multiple regression analysis. The result of this stage is the following prediction equation:

$$C_p = B_0 + B_1 R_{\lambda 1} + B_2 R_{\lambda 2} + \ \ldots\ldots\ B_n R_{\lambda n} \tag{1}$$

where $C_p$ stands for the predicted property value, $B_0$ is a constant coefficient for the current population, $B_1 - B_n$ are coefficients for each wavelength reading, $R$ is the reflectance or its manipulation (e.g. first or second derivatives) and $\lambda$ stands for wavelength. The prediction accuracy is judged by using the following equation:

$$SEC = \sqrt{\Sigma (C_a - C_p)^2/(n-1)} \tag{2}$$

where $C_a$ stands for the laboratory values and $n$ for the number of samples involved in the analysis. In general equation (1) is empirically extracted from a spectrally and chemically known population and is known as a calibration set.

## 3. Results

Table 1 provides general information about the selected soil population as obtained from the laboratory analytical data (minimum {MIN} maximum {MAX}, standard deviation {SD}, and the coefficient of variance {CV}). From this table it can be seen that a wide range of both organic matter and EC (and hence soil salinity) values does exist. The relatively high values of organic matter (MIN = 3.56%) occur because most of the analysed soils were characterized by high contamination of dry vegetation debris (the soils were not run through a $>2$ mm sieve as is routinely done in soil science prior to soil analysis). The electrical conductivity (EC) values range from 0.59 dsm cm$^{-1}$ (MIN) to 27.4 dsm cm$^{-1}$ (MAX) with a mean value of 4.14 dsm cm$^{-1}$ (AVE). The relatively high EC values provide evidence that the soil surface areas along the study location were affected by salinity contamination. This finding stands in good agreement with field observations, which show significant soil degradation in several locations around agricultural fields. The soil saturated moisture (SM) values are relatively lower than expected from clayey soils (AVE of 43.31%). However, because the final moisture stage in this method is subjective, the most important issue is that all soils were treated equally. Other properties (soil field moisture {FM}, and pH {PH}) represent normal values for the soils examined at this time of the year.

The VNIRA procedure was first run on the laboratory spectral data (48 soil samples and their spectra) to obtain a correlation between the spectral and the chemical data (calibration stage). This step was taken in order to ensure that the selected populations have reliable chemical and spectral relationships to perform a confident VNIRA analysis. Doing so revealed a significant ability to predict each soil property from its reflectance information. In table 2 some statistical parameters of the laboratory VNIRA results are provided (marked with @). In the next stage, the DAIS spectral data (over the 0.5–2.3 $\mu$m spectral range) were processed using the VNIRA approach and two spectral manipulations: the original DAIS reflectance ($R$) and its first derivative ($R'$). The first step for each spectral domain was to generate

Table 1. General information about each property as obtained from the wet-chemistry analyses.

| | FM Field moisture content (%) | OM Organic matter (%) | PH pH | EC Electric conductivity (Deci Simens (cm$^{-1}$) | SM Soil-saturated moisture (%) |
|---|---|---|---|---|---|
| Average | 9.08 | 4.83 | 7.9 | 4.14 | 43.31 |
| Std. Dev. | 6.79 | 0.70 | 0.1 | 6.21 | 2.77 |
| CV*(%) | 74.8 | 14.4 | 1.2 | 150 | 6.4 |
| Minimum | 4.67 | 3.56 | 7.5 | 0.59 | 37.98 |
| Maximum | 28.10 | 7.04 | 8.2 | 27.40 | 48.93 |
| Average | 9.08 | 4.83 | 7.9 | 4.14 | 43.31 |

Std. Dev. = Standard deviation, CV(%) = Coefficient of variation (Std. dev. *100/Average).

Table 2. The calibration equations obtained for each property (see text for more details).

| Property | SEC, SEP, SEL | $R_m^2$ | Prediction equation | Assignments |
|---|---|---|---|---|
| Soil Field Moisture (FM) | 0.045, 0.14, 0.016<br>0.027@ | 0.645<br>0.847@ | R_0.739 μm*0.378179 + R_1.65 μm*0.389602-<br>R_0.689 μm*0.184370 + 0.062336 | 1.65 μm-reflectance slope<br>0.688 μm-reflectance slope<br>0.739 μm-reflectance slope/chlorophyll |
| Organic Matter (OM) | 0.003, 0.015, 0.002<br>0.0012@ | 0.827<br>0.837@ | R_0.722 μm*0.135211 + R_2.328 μm*0.034358-<br>R_0.705 μm*0.117264 + R_1.678 μm*0.017276 + 0.052084 | 0.722 μm-chlorophyll remaining<br>1.678 μm-C-H in cellulose<br>2.328 μm-Humic acid, Pectin, Lignin |
| Soil-Saturated Moisture (SM) | 0.019, 0.021, 0.005<br>0.0006@ | 0.759<br>0.81@ | R_2.085 μm*0.136384 + R_2.314 μm*0.081181 +<br>R_2.183 μm*0.220235-R_1.563 μm*0.2380-<br>R_1.538 μm*0.115681 + 0.500373 | 2.085 μm–adsorbed water OH<br>2.183 μm-OH combination of $\upsilon + \delta$ in clay mineral lattice<br>1.538, 1.563 μm-OH combination of $2\upsilon$ in clay mineral lattice |
| Electrical Conductivity (EC) | 4.36, 4.58, 0.1<br>2.57@ | 0.665<br>0.874@ | R_0.739 μm*28.936957 + R_1.65 μm*50.257661-<br>R_2.166 μm*26.44311-7.19963 | 0.739 μm-organic-matter assignments<br>1.65 μm-adsorbed water OH<br>2.166 μm-adsorbed water OH |
| PH | 0.146, 0.26, 0.1<br>0.073@ | 0.528<br>0.883@ | R_0.722 μm*0.517083 + R_2.118 μm*0.730835 +<br>8.040777 | Not determined |

wl stands for the wavelength (μm) in the equation. SEC $= \sqrt{\{\{\Sigma\,(C_m - C_p)\}^2/n\}}$ where $C_x$ is the constituent values in the measured ($x = m$) and predicted ($x = p$) domains. @ stands for values obtained from running the VNIRA procedure on laboratory data (spectral and chemistry). $R_m^2$ is a multiple regression coefficient. SEP $= \sqrt{\{\Sigma\,(C_m - C_p)\}^2/n\}}$ where $C_x$ is the constituent values in the measured ($x = m$) and predicted ($x = p$) domains in samples were not involved in the calibration procedure. SEL $= \sqrt{\{\Sigma\,\Sigma\,(C_{ni} - AVE_i)\}^2/n_i\}}$ where $n$ refers to a single analytical measurement in the laboratory of sample $i$ and $AVE_i$ is the average of all replications of sample $i$.

the correlogram spectrum in order to judge whether the highest correlated wavelengths consisted of reliable spectral assignments (known from the literature). This step is extremely important because it is intended to prevent spectral noise from entering into the analyses (known as an overfitting problem, Davies and Grant 1987). Figure 2 provides the correlograms used for all properties examined under the first derivative spectral domain. As seen, a relatively high correlation exists in several wavelengths between the properties in question and their spectral readings ($r \cong 0.5 - 0.6$). In the case of organic matter for example, all of these wavelengths can be assigned according to Ben-Dor *et al.* (1997) to remaining chlorophyll (around 0.7 $\mu$m), oil and cellulose (around 1 $\mu$m), pectin, starch and cellulose (around 1.6 $\mu$m), and lignin and humic acid (around 2.3 $\mu$m). The prediction equations extracted from these correlograms are given in table 2. These equations were generated by calculating a forward stepwise multiple analysis on the highest 38 spectral reliable bands. The next step was to run the best equation on a pixel-by-pixel basis on the DAIS reflectance cube in order to produce a spatial view of the property in question (see later discussion). In table 2, the prediction (calibration) equations for the examined soil properties are given along with some statistical parameters ($R^2_m$ , SEC, SEP, and SEL; see definitions in table 2) and possible spectral assignments. From table 2 it can be seen that in general, the prediction performances obtained for soil field moisture, organic matter, saturated moisture, and soil salinity (EC) are favourable ($R^2_m > 0.65$). Both the organic matter and the field moisture properties are 'features' properties (having significant spectral assignments, which are also termed 'chromophores'). In organic matter, many features across the VIS-NIR-SWIR regions are dominant because of the many functional groups active in this spectral region (see previous discussion).

In order to determine whether the wavelengths were spectrally reliable, we generated a pure spectra library of components representing the soil environment of Zvaim Valley resampled into the DAIS spectral configuration. Figure 3 (*a*, *b*, *c*) provides the spectra of the following components: silt-loam soil in six different

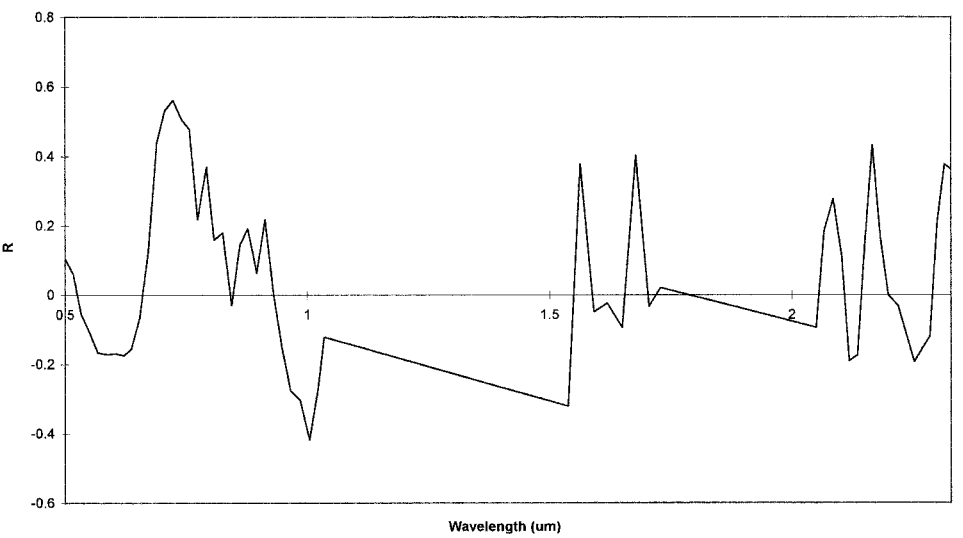


Figure 2. The correlograms of all examined properties as obtained from the first derivative of the reflectance DAIS readings (R′) and the laboratory values.

moisture contents ranging from 0.8% to 20.2% (taken from Bowers and Hanks (1965) figure 3(*a*)); montmorillonite, kaolinite, halite, illite and quartz (taken from JPL-spectral library, Grove *et al.* 1992 figure 3(*b*)) and pure (fresh-*a* and decomposed-*b*) organic matter (taken from Ben-Dor *et al.* 1997, figure 3(*c*)). From figure 3(*a*) it can be postulated that in addition to peak intensity changes at around 1.9 $\mu$m (assigned to OH in water; see montomorillonite spectrum) and at 2.2 $\mu$m (assigned to OH in clay lattice; see montmorillonite spectrum), significant and consistent changes of the spectral slope along the VIS-NIR (0.5–1.3 $\mu$m), SWIR-I (1.55–1.8 $\mu$m) and SWIR-II (2.25–2.4 $\mu$m) regions also exist. As Ben-Dor and Banin (1994) pointed out, the strong OH bands at 1.4 $\mu$m and 1.9 $\mu$m may not be always correlated with soil/clay moisture. Ben-Dor and Banin (1994) showed that across the NIR-SWIR spectral region (using 25 bands), the 2.365 $\mu$m wavelength is highly correlated with hygroscopic moisture, which emerged from the slope changes. In this regard it is interesting to note that using 63 bands across this region with the same population, the 1.621 $\mu$m wavelength is best for predicting soil moisture status based on a similar slope assignment (Ben Dor 1992). As seen in table 2, the selected bands for predicting soil moisture are 0.739, 0.86, and 1.65 $\mu$m, which all fell within the spectral range of 'VIS-NIR slope changes' previously discussed. Because these slope changes (in the original spectra) are more pronounced in the first derivative domain, these wavelengths can be assigned to the slope-water relationship. Nevertheless, we suspect that the 0.739 $\mu$m wavelength is also assigned to chlorophyll absorption that might occur because of organic matter/vegetation remaining in the soil (see the pure organic matter spectra in figure 3(*c*) or even to microphytes (Karnieli and Tsoar 1994). In general, relatively high organic matter content will be found along areas of relatively high moisture. In the current study the coefficient of determination value obtained between organic matter and soil moisture (table 3) is relatively low ($r = 0.37$), but still high enough to indicate that such a trend might exist. To validate the above discussion for the Zvaim soil samples, figure 4 gives laboratory, field and airborne spectra of two representative soil samples. As can be clearly seen, the absorption features of OH in clay lattice (around 2.2 mm) and in adsorbed water (around 1.9 $\mu$m) are significant together with noticeable slopes at around the VIS (0.4–1.0 $\mu$m) and at the SWIR-1 (1.2–1.8 $\mu$m) spectral regions. Weak spectral features can be depicted around 0.7 $\mu$m and 0.83 $\mu$m, which can be attributed to both organic matter remaining and iron oxide components in these soils, respectively.

## 4. Discussion

As Ben-Dor and Banin (1995b) pointed out, 'featureless' properties (properties without a direct chromophore) may also be predicted via internal correlation with

Table 3. The correlation matrix of the wet chemistry components.

| | SM | FM | OM | PH | EC |
|---|---|---|---|---|---|
| SM | 1.00 | | | | |
| FM | 0.29 | 1.00 | | | |
| OM | 0.19 | 0.37 | 1.00 | | |
| PH | −0.22 | −0.26 | −0.39 | 1.00 | |
| EC | 0.21 | 0.58* | 0.43$^{+}$ | −0.61 | 1.00 |

SM = Saturated Moisture, FM = Field Moisture, OM = Organic Matter, PH = pH, EC = Electrical Conductivity of the soil extracted pasta liquids.

*, $^{+}$ Significance at the 0.001 and 0.01 probability level, respectively.

'chromophoric' properties. In this case, neither the soil salinity nor the pH has any direct spectral assignments. However, soil salinity (EC) is significantly correlated with field moisture content as seen in table 3 ($r = 0.58$), and hence its prediction equation consists of the field moisture assignments. From the correlation coefficient matrix it is postulated that a negative correlation exists between pH and EC ($r = -0.61$), whereas no direct correlation exists between pH and field moisture or organic matter ('chromophoric') properties. If a more varied population containing acidic, alkaline and neutral soils was involved, it is possible that a prediction equation could be obtained for the pH property based on internal correlation. Also it may be possible that a secondary intercorrelation (pH via EC with FM) might be less effective than the primary intercorrelation (EC with FM). The saturated moisture (SM) content is known to be significantly correlated with clay mineralogy and content (Banin and Amiel 1970). As the clay content and its specific surface area increase (e.g. appearance of montmorillonite as the dominant clay mineral in these soils), more water molecules may enter into the final stage of the soil-saturated mixture and hence affect the saturated moisture content. Thus the assignment of the saturated moisture wavelengths in table 2 are of OH in clay mineral lattice at 1.563 $\mu$m, 1.538 $\mu$m ($\upsilon + 2\delta$) and 2.183 $\mu$m ($\upsilon + \delta$) and of water OH at 2.085 $\mu$m. In summary it can be said that reliable spectral models for soil field moisture, organic matter content, soil saturated moisture and soil salinity were achieved from the DAIS data. The reliability is based on both statistical parameters and spectral assignments. In general, quantification (and detection) of soil salinity is a difficult and challenging task using reflectance data (Csillage *et al.* 1993) or images based on sun radiation if the effect is not significant to the human eye (Metternicht and Zinck 1997). This is because possible salts in the soil (e.g. NaCl), do not consist of significant absorption peaks across the relevant spectral region (see for example the spectrum of halite in figure 3(*b*)). In this case an indirect correlation with soil field moisture (and less with organic matter) enables the VNIRA-salinity measurements to be effective. The correlation between soil field moisture and soil salinity in this area has to be considered: in the study area, soil salinity emerges because of a high groundwater table causing a capillary rise driven by the evaporation process. This causes the formation of salt crusts at the soil/atmosphere interface (visible or invisible). Along salinity-infected areas, the field moisture is relatively high, and hence, the VNIRA analysis significantly picks its location via the field moisture assignments. In reality, the groundwater level may change from one season to another, and the saline crust might serve as an indicator for determining its spatial dynamics.

Figure 5 illustrates the 'property images' as generated by applying the prediction equations (see table 2) on a pixel-by-pixel basis. Basically it is assumed that an 8 m $\times$ 8 m pixel can show mixed effects of the property in question. However, although this area may be represented by a diverse distribution, the calculated value may be a fair average to demonstrate as precisely as possible the spatial distribution of the soil property.

In general it can be seen that a reliable image of each property is depicted (excluding the covered vegetation pixels, which are masked out of the image). This conclusion is based on a priori knowledge of the area as well as on a careful validation check of five independent soil samples. These samples were analysed in the laboratory, just like the samples used for the calibration step, and are termed the validation set. In this set, the VNIRA-based values were extracted from the quantitative images obtained in the previous step. The predicted values were then

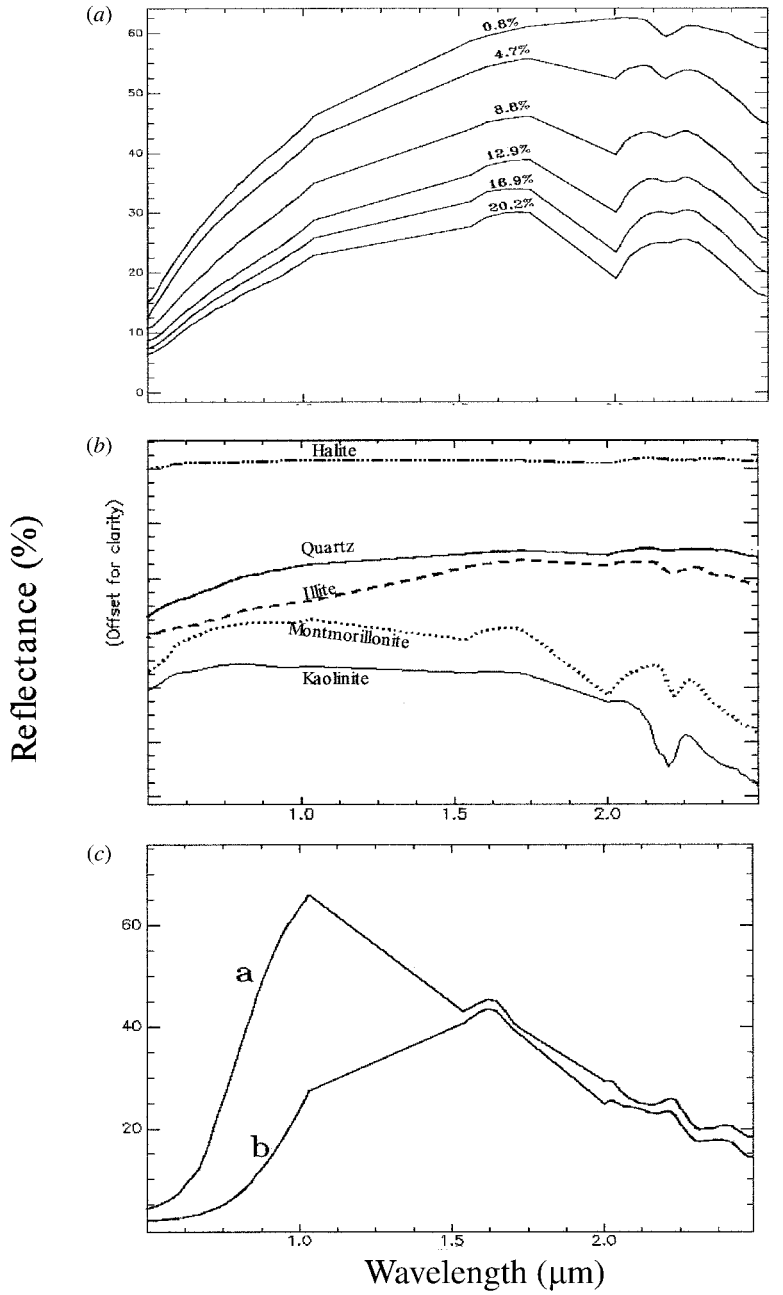


Figure 3. Several pure materials suspected to be in the soil samples resampled into the DAIS spectral configuration (*a*) a silt-loam soil with varying hygroscopic moisture, taken from Bowers and Hanks 1965, (*b*) minerals taken from Grove *et al.* 1992 and (*c*) organic matter at two different composition stages (a = fresh, b = decomposed after 355 days), after Ben-Dor *et al.* 1997.

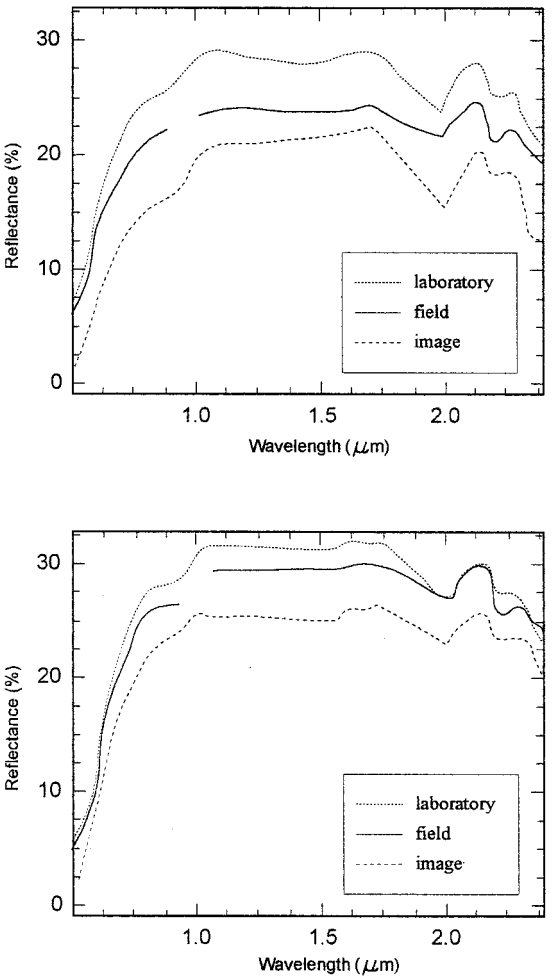


Figure 4. Representative spectra (laboratory, field and airborne) of two soil samples, representing typical spectral features emerging from a mixture of suggested pure chromophores given in figure 3.

compared with the actual (laboratory) values, and the results are presented in figure 6. It appears that a favourable relationship occurs between the two values except for sample b26. For practical reasons, the DAIS spectrum of sample b26 could not be properly spatially extracted. This sample was located between two cotton plots significantly influenced by a mixed (soil and vegetation) pixel problem (a problem might arise in any non-homogeneous pixel environment). It is obvious that the b26 sample is an outlier sample among the validation set population. In general, heterogeneity in the population examined by the VNIRA approach may produce outliers (Ben-Dor and Banin 1990). In this regard it is very important to identify the outliers prior the calibration stage so that the selected model is stable and reliable. This step was taken for sample b26 in the calibration stage, which is independent of the validation stage. The poor validation results obtained from sample b26 demonstrate that exact spatial identification and positioning of samples in the VNIRA technique are critical. It should be noted that the prediction equations developed in this study

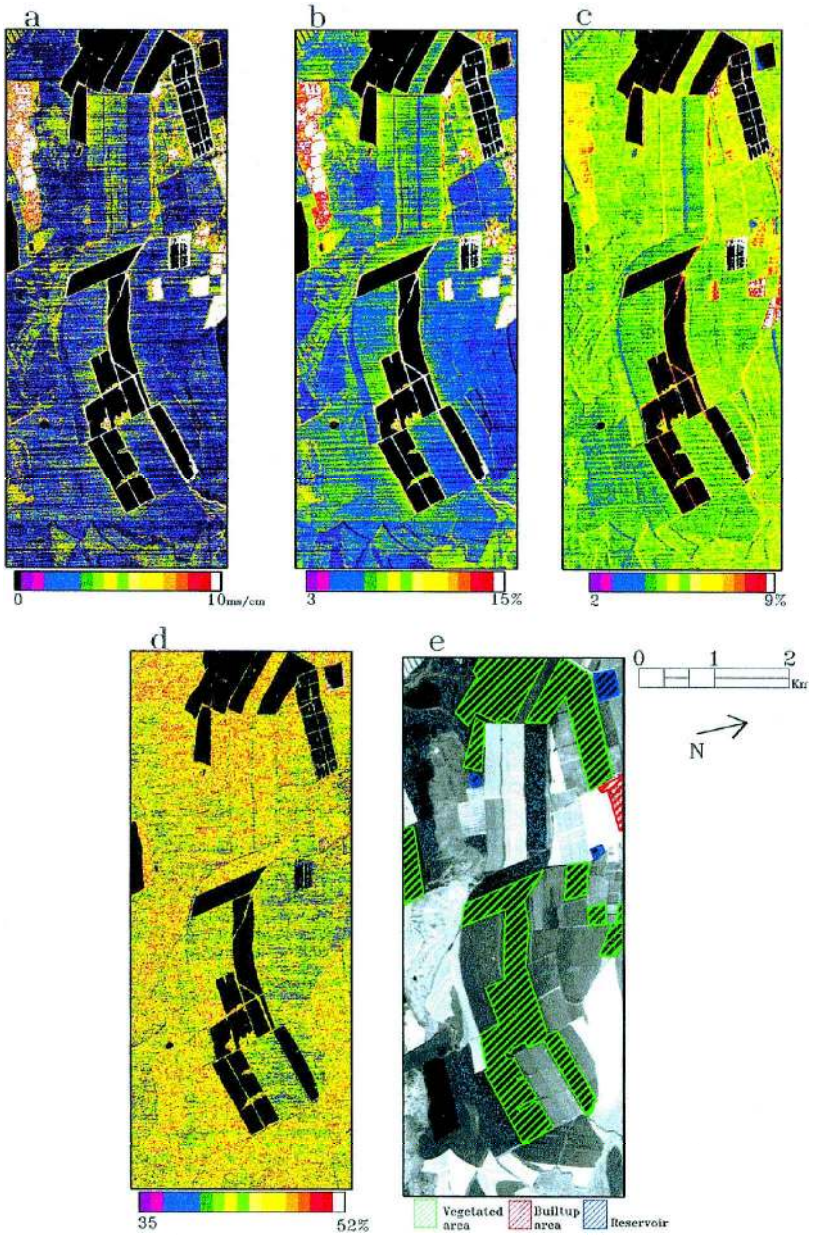


Figure 5. A mosaic image providing the spatial distribution of soil properties after applying the prediction VNIRA equation given in table 2 to the DAIS reflectance cube. Each image is a spatial subset representing the intensive agriculture areas along the selected flight line. (*a* = Electrical Conductivity (EC), *b* = Field Moisture (FM), *c* = Organic Matter (OM), *d* = Saturated Moisture (SM), *e* = Reference base map {channel #12 0.767 $\mu$m})

are adequate only for the soil population examined in this study, i.e. representing the soil types of the calibration set.

It can be concluded that although a vast field validation check has not been

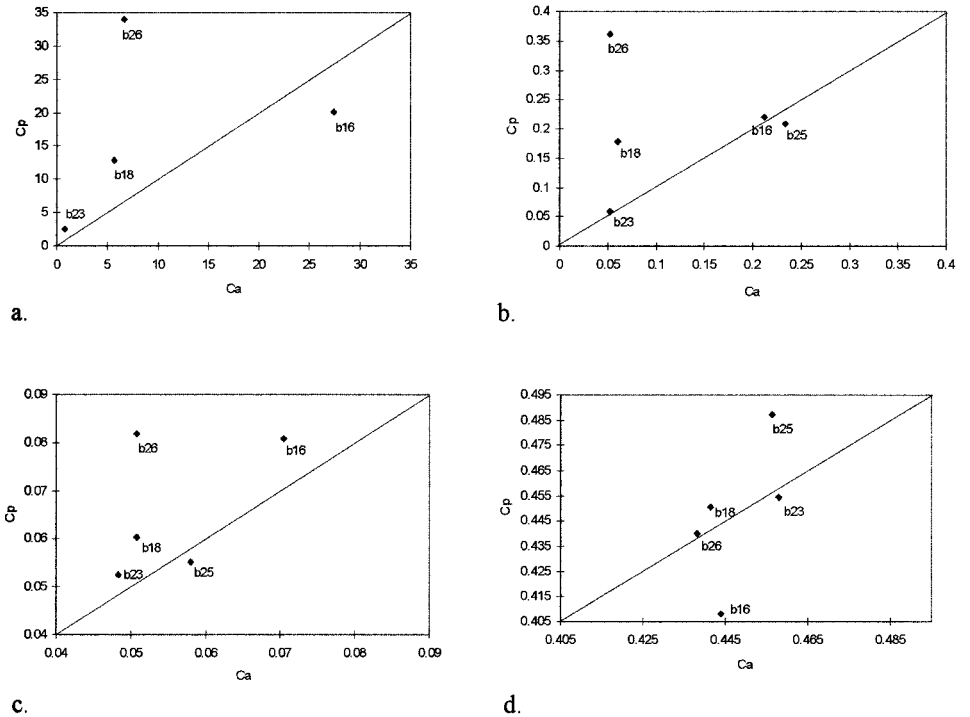


Figure 6. Validation plots of each examined property, showing the actual values of selected soil samples along the study area against the predicted values extracted from the VNIRA image (a = EC (Ds $cm^{-1}$); b = FM (fraction); c = OM (fraction); d = SM (fraction)).

performed on a large scale, the current results do indicate that the VNIRA methodology is a feasible tool for quantitatively assessing soil properties using a remote-sensing means. It is important to note that the quality of the DAIS-7915 data still lags (in terms of signal-to-noise ratio, radiometric calibration and sensors' stability) far behind that of laboratory data and even other airborne HSR data, such as the AVIRIS 97 or HyMap data (Green *et al.* 1997, Cocks *et al.* 1998 ). Although the results obtained in this study are promising, we strongly believe that using better HSR data could improve the VNIRA's accuracy and could enable it to be used as an alternative tool for soil surface mapping. Another limitation is the fact that optical remote sensing can directly assess only the soil surface area. Because full and detailed soil mapping must consist of the entire profile, this tool is not optimally sufficient for traditional soil mapping. Nevertheless, it is a most useful vehicle for assessing the properties of surface conditions (e.g. physical crust) or significant properties on the surface (e.g. soil organic matter or surface moisture). In conclusion it can be summarized that in spite of the above-mentioned limitations, the current DAIS-7915 enabled reliable and quantitative assessment of soil properties on the soil surface. The feasibility of the DAIS-7915 data to be processed by the VNIRA methodology demonstrates that this analytical step can be practically used on other HSR data, which is acquired by a better HSR sensor.

## 5. Soil property maps

Two major limitations were encountered with optical remote sensing of soils: (1) it is impossible to sense the entire soil profile (see previous discussion); and (2) soil vegetation (dry or green) masks out Sun photons, preventing interaction with the soil. Taking the second limitation into account, it appears that along densely vegetated areas (temporary or permanent) no soil information can be extracted from the HSR images in general and from quantitative VNIRA images in particular (Murphy and Wadge 1994, Zhang *et al.* 1998). In advanced agriculture it is important to know the soil status in order to improve decision making from one season to another. Because the soil surface is not always clear of vegetation coverage, a reliable spatial mapping technique for soil properties is strongly required. In this regard, we suggest application of an interpolation process on non-vegetated sites in order to estimate the entire area (vegetated and non-vegetated). For that purpose and to increase spatial accuracy, it is important to have a large number of soil samples for the analysis. Traditionally, preparation of such a set (based on field and laboratory work) is a time- and money-consuming process and is not always possible. Alternatively, the VNIRA images offer a favourable database from which large numbers of soil samples and their corresponding properties can be rapidly extracted. Accordingly, and based on the quantitative images created in the previous stage, we randomly selected approximately 80 soil targets (pixels from the VNIRA image with their corresponding soil property values) from an area measuring 49 km$^2$. Figure 7 shows the exact locations of these sites with polygons overlain to represent areas of vegetation coverage. Examining the histogram of the chosen soil population (Gaosian like) along with its spatial distribution (homogeneous like) suggests that the selected group is a favourable database within which the selected interpolation processes can be run. The final product of this stage is intended to be geocoded maps with isovalue

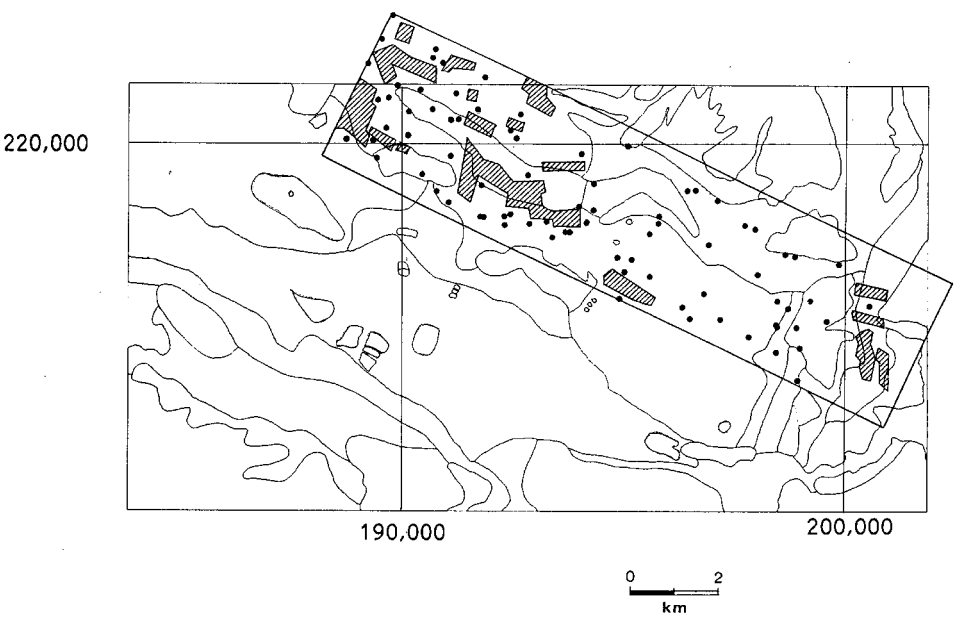


Figure 7. Locations of the interpolation points taken for the IDW analysis. Overlain are polygons representing the areas of vegetation coverage.

vectors for each property. The interpolation procedure selected for this stage was the Inverse Distance Weighting Interpolation (IDW). This technique serves as a model in the MapInfo software (MapInfo User's Guide 1996) and is a type of moving average interpolative usually applied to highly variable data. For certain data types it is possible to return to the collection site and record a new value that is statistically different from the original reading, but within the general trend for the area. Because this method is recommended for soil chemistry results, bedrock assays and monitoring environmental data we used it in this study. The IDW technique calculates a value for each grid node by examining surrounding data points that lie within a user-defined search radius. The node value is calculated by averaging the weighted sum of all the points. Data points that lie progressively farther from the node influence the computed value far less than those closer to the node. Using the 80 soil samples, the IDW technique was run to provide the soil property maps that are presented in figure 8(*a*, *b*, *c*, *d*). In general, good spatial agreement exists between the EC (soil salinity) and the field moisture content maps (figures 8(*a*) and (*b*), respectively). This was expected based on the relationships already obtained between the laboratory values of these properties (table 3) as well as the positive agreement that occurred between their spectral assignments (table 2). Comparing the organic matter map (figure 8(*c*)) with both the EC and the field moisture maps reveals that some areas are highly correlated (e.g. at the north-west edge) and some areas are not (e.g. at the centre and south-east edge). A partial validation check of the EC (salinity) on the IDW + VNIRA map discovered new saline spots, as seen in figure 8(*b*) and represented by three yellow polygons north of Hamadia farms (situated in the south-east corner of the area), which were verified on the ground. Although a comprehensive validation check has not been performed, the previous ground validation checks strongly suggest that the IDW + VNIRA methodology is a feasible tool for agriculture applications. It is assumed that improved data quality and improved data processing would provide even better results. Accordingly, it is hoped that this paper can act as a precursor to further implementation of the VNIRA methodology in soil mapping applications using many varieties of HSR data. The VNIRA approach can take place together with the ongoing development of the HSR technology, which aims at providing an advanced spatial sensor with relatively high spectral, spatial and temporal resolutions.

## 5. Summary and conclusions

This study employs the laboratory approach known as VNIRA for soil mapping applications by using DAIS-7915 hyperspectral data. The VNIRA method uses a spectral-chemical empirical model to predict soil properties from their reflectance spectra only. This is done by using a well-known set of calibration data and an unknown set of validation data to check the results. Under remote sensing conditions this approach has never been examined for soil applications. This paper could therefore serve as a case study from which other HSR users can start in order to create quantitative soil surface maps. In this regard many problems arose, such as atmospheric contamination of the raw data, low signal-to-noise ratios, unreliable spectral band response and positioning of the sample on the ground. Although effort was made to overcome all of these difficulties, the results were still affected by these obstacles and the process thus lagged in comparison with laboratory accuracy. Using the DAIS spectral information it was possible to obtain reliable prediction equations for the following soil properties: soil moisture, soil salinity (EC), soil saturated

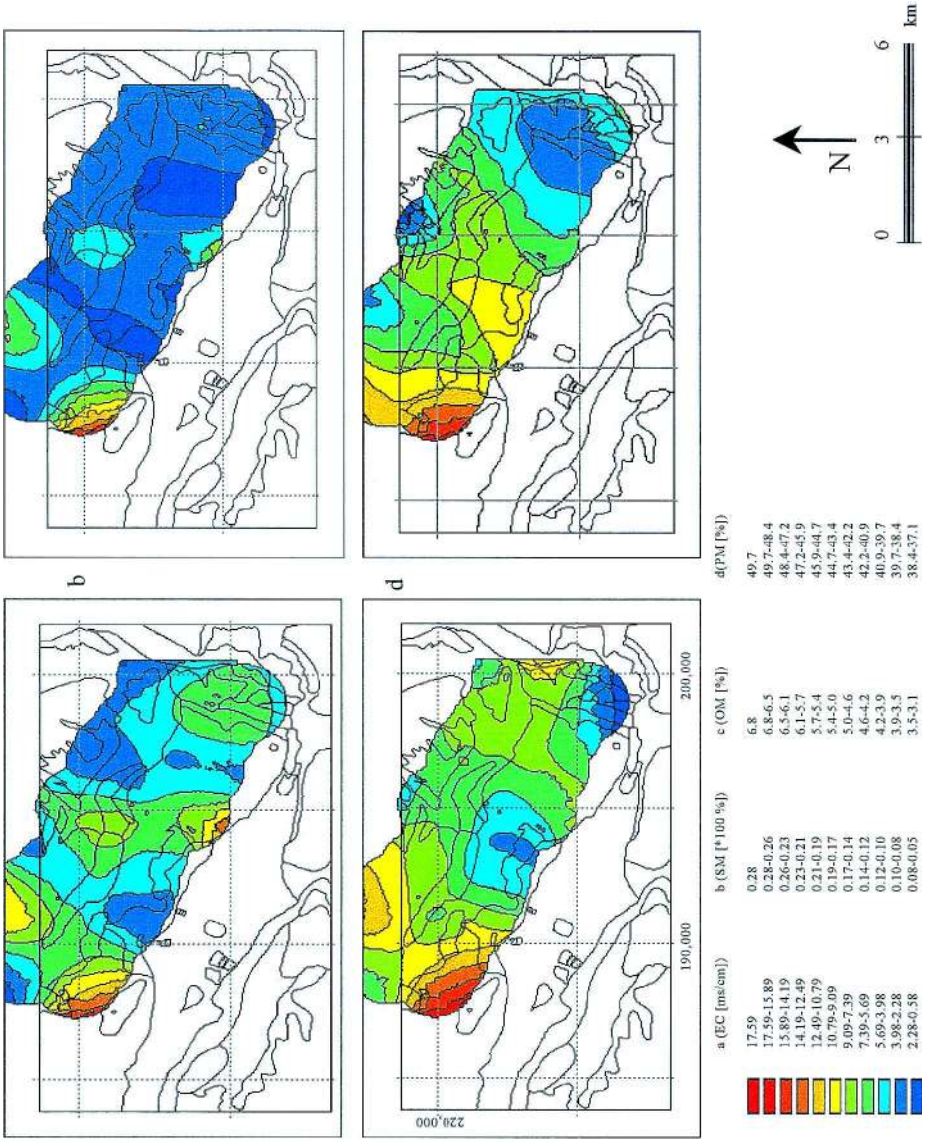


Figure 8. A mosaic image (rectified to local Israeli net coordinates) providing the spatial distribution of each property after application of the IDW interpolation technique (see text for more details). ($a$ = Electrical Conductivity (EC), $b$ = Field Moisture (FM), $c$ = Organic Matter (OM), $d$ = Saturated Moisture (PM)).

moisture and organic matter content. It was found that the intercorrelation between properties is as important a parameter as the spectral information. This is because the intercorrelation enlarges the envelope of spectral assignments and provides a greater physical basis for the spectral prediction model. In this regard it was found that although the soil salinity (EC) is a featureless property, it can be spectrally explained via field moisture assignments.

There was an indication that organic matter assignments played a role in the soil field moisture assignments. A validation stage using five independent samples yielded reasonable results (except for one outlier, which was questionable in terms of its ground positioning). This stressed the fact that a careful positioning of ground targets using the VNIRA approach under a remote-sensing domain is essential. An attempt to estimate soil property distribution under vegetation coverage using the VNIRA results was made. For that, we employed a random selection of 80 soil samples from the quantitative images and applied an interpolation technique to provide an isocontour map for each of the studied soil properties. It was shown that merging the quantitative remote sensing (VNIRA) technique with a spatial interpolation algorithm (IDW) provides a useful tool for soil mapping applications. Although the results are still far from what can be achieved in the laboratory, the study showed that the VNIRA technique is a feasible tool for mapping soil properties using HSR data. Better HSR data, more soil samples and sharpening the VNIRA approach could be the combination that makes this method fully applicable.

## Acknowledgments

This study was supported by the KKL, Land Development Authority (under CHOSEN internal fund) and by the German Israel Foundation (GIF). The DAIS-7915 overflight was funded by the European Community. We are grateful to the DLR Optoelectronics Department for their efforts in bringing the sensor to Israel and for conducting the air campaign under very high standards.

## References

Banin, A., and Amiel, A., 1970, A correlation of the chemical physical properties of a group of natural soils of Israel. *Geoderma*, **3**, 185–198.

Ben-Dor, E., 1992, The light reflectance in the visible and near infrared region (0.4–2.5 $\mu$m) of selected Israeli soils and its correlation with physical-chemical properties of the soils. A PhD dissertation, submitted to the Hebrew University of Jerusalem July 1992, in Hebrew (English abstract).

Ben-Dor, E., and Banin, A., 1989, Determination of organic matter content in arid-zones soils using simple loss-on-ignition method. *Communications in Soils Science and Plant Analysis*, **20**, 1675–1695.

Ben-Dor, E., and Banin, A., 1990, Near infrared reflectance analysis of carbonate concentration in soils. *Applied Spectroscopy*, **44**, 1064–1069.

Ben-Dor, E., and Banin, A., 1994, Visible and near infrared (0.4–1.1 $\mu$m) analysis of arid and semiarid soils. *Remote Sensing of Environment*, **48**, 261–274.

Ben-Dor, E., and Banin, A., 1995a, Near infrared analysis (NIRA) as a rapid method to simultaneously evaluate, several soil properties. *Soil Science Society of America Journal*, **59**, 364–372.

Ben-Dor, E., and Banin, A., 1995b, Near infrared analysis (NIRA) as a simultaneous method to evaluate spectral featureless constituents in soils. *Soil Science*, **159**, 259–269.

Ben-Dor, E., Inbar, Y., and Chen, Y., 1997, The reflectance spectra of organic matter in the visible near infrared and short wave infrared region (400–2500 nm) during a controlled decomposition process. *Remote Sensing of Environment*, **61**, 1–15.

Berk, A., Bernstein, L. S., and Robertson, D. C., 1989, MODTRAN: A moderate resolution model for LOWTRAN7. Final report, GL-TR-0122, AFGL, Hanscom AFB, MA.

Bowers, S. A., and Hanks, R. J., 1965, Reflectance of radiant energy from soils. *Soil Science*, **100**, 130–138.

Clark, R. N., King, T. V. V., Klejwa, M., Swayze, G., and Vergo, N., 1990, High spectral resolution reflectance spectroscopy of minerals. *Journal of Geophysics*, **95**, 12 653–12 680.

Cocks, T., Jrnssen, R., Stewart, A., Wilson, I., and Shields, T., 1998, The HyMap™ airborne hyperspectral sensor: The system, calibration and performance. In *Proceedings of the 1st EARSeL Workshop on Imaging Spectroscopy*, *Zurich*, *Switzerland* (Paris: ERSEL), pp. 37–42.

Csillage, F., Pasztor, L., and Biehl, L. L., 1993, Spectral band selection for the characterization of salinity status of soils. *Remote Sensing of Environment*, **43**, 231–242.

Curran, P. J., Dungam, B. A., Macler, S. E., Plummer, and Peterson, D. L., 1992, Reflectance spectroscopy of fresh whole leaves for the estimation of chemical concentration. *Remote Sensing of the Environment*, **39**, 153–166.

Dalal, R. C., and Henry, R. J., 1986, Simultaneous determination of moisture, organic carbon and total nitrogen by near infrared reflectance spectroscopy. *Soil Science Society of America Journal*, **50**, 120–123.

Davies, A. M., and Grant, A., 1987, Review: near infrared analysis of food. *International Food Science and Technology*, **22**, 191–207.

Gao, B. C., and Goetz, A. F. H., 1990, Column atmospheric water vapor and vegetation liquid water retrievals from airborne imaging spectrometer data. *Journal of Geophysical Research*, **95**, 3549–3564.

Gao, B. C., and Goetz, A. F. H., 1995, Retrieval of equivalent water thickness and information related to biochemical components of vegetation canopies from AVIRIS data. *Remote Sensing of Environment*, **52**, 155–162.

Gao, B. C., Heidebrecht, K. B., and Goetz, F. H. A., 1993, Derivation of scaled surface reflectances from AVIRIS data. *Remote Sensing of Environment*, **44**, 165–178.

Gardner, W. H., 1986, *Water content in methods of soil analysis*, part 1. edited by R. Klute, (Madison, WI: Soil Society of America), pp. 493–541.

Goetz, A. F. H., Vane, G., Solomon, J. E., and Rock, B. N., 1985, Imaging spectroscopy for Earth remote sensing. *Science*, **228**, 1147–1153.

Green, A. A., Berman, M., Switzer, P., and Craig, M. D., 1988, A transformation for ordering multispectral data in terms of image quality with implications for noise removal. *IEEE Transactions on Geoscience and Remote Sensing*, **26**, 65–74.

Green, R. B., Pavri, B., Faust, J., Williams, O., and Chovit, C., 1997, Inflight validation of AVIRIS calibration in 1996 and 1997. In *Proceedings of the Airborne Visible/Infrared Imaging Spectrometer (AVIRIS)* (Pasadena: JPL Publications), pp. 193–203.

Grove, C. I., Hook, S. J., and Paylor, E. D., II, 1992, *Laboratory reflectance spectra of 160 minerals, 0.4 to 2.5 micrometer* (Pasadena: JPL Publication 92-2).

Hausknecht, P., Flack, J. C., Huntington, J. F., Mason, P., and Boardman, J. W., 1999, Hyperspectral profiling versus imaging: A mineral mapping case study to evaluate the oars concept. In *Proceedings of the Thirteenth International Conference on Applied Geologic Remote Sensing*, *Vancouver and Canada 1–3 March 1999*, pp. 529–536.

Karnieli, A., and Tsoar, H., 1994 Spectral reflectance of biogenic crust developed on desert dune sand along the Israel-Egypt border. *International Journal of Remote Sensing*, **16**, 369–374.

Keller, P. A., Keller, I., and Itten, K. I., 1998, Combined hyperspectral data analysis of an alpine lake using CASI and DAIS7915 Imagery. In *1st EARSeL Workshop on Imaging Spectroscopy*, *Zurich*, *Switzerland 6–8 October 1998* (Paris: EARSEL), pp. 237–243.

Kruse, F. A., 1988, Use of airborne imaging spectrometer data to map minerals associated with hydrothermally altered rocks in the northern Grapevine Mountains, Nevada and California. *Remote Sensing of Environment*, **24**, 31–51.

Kruse, F. A., Kierein-Young, K. S., and Boardman, J., 1990, Mineral mapping at Cuprite, Nevada, with 63 channel imaging spectrometer. *Photogrammetric Engineering and Remote Sensing*, **56**, 83–92.

Lacapra, V. C., Melack, J. M., Gastil, M., and Valeriano, D., 1996, Remote sensing of foliar chemistry of inundated rice with imaging spectroscopy. *Remote Sensing of Environment*, **55**, 50–58.

Lazar, M., Ben-Avraham, Z., and Ben-Dor, E., 1998, Comprehensive comparison of atmospheric corrections of CASI hyperspectral images over water: A case study. In *Proceedings of 1st EARSeL Workshop on Imaging Spectroscopy, Zurich, Switzerland 6-8 October 1998* (Paris: EARSEL), pp. 97–103.

Lorcher, G., 1999, Mapping of hydrothermal alteration from AVIRIS data using spectral analysis tools and spectral libraries. In *Proceedings of the Thirteenth International Conference on Applied Geologic Remote Sensing, Vancouver BC. Canada 1–3 March 1999* (Ann Arbor, MI: ERIM), pp. 359–362.

Mapinfo User's Guide, 1996, Vertical mapper contour modeling and display software. Desktop mapping software.

Martin, M. E., and Aber, J. D., 1993, Measurements of canopy chemistry with 1992 AVIRIS data at Blackhawk Island and Harvard Forest. In *Summaries of the 4th Annual JPL Airborne Geoscience Workshop 25–29 October 1993* (Pasadena: JPL Publications), 113–116.

Mettnicht, G., and Zinck, J. A., 1997, Spatial discrimination of salt- and sodium-affected soil surfaces. *International Journal of Remote Sensing*, **18**, 2571–2586.

Muller, A., and Ortel, D., 1997, DAIS Large-scale facility, the DAIS-7915 imaging spectrometer in a European frame. In *Proceedings of the Third International Airborne Remote Sensing Conference and Exhibition, Copenhagen, Denmark* (Ann Arbor, MI: ERIM), **II**, 684–691.

Murphy, R. J., and Wadge, G., 1994, The effect of vegetation on ability to map soils using imaging spectrometer data. *International Journal of Remote Sensing*, **15**, 63–86.

Norris, K. H., 1988, History and present state and future prospects for near infrared spectroscopy. In *Analytical Applications of Spectroscopy,* edited by C. S. Creaser and A. M. C. Davies (London: Royal Society of Chemistry), pp. 33–91.

Peng, W., 1998, Synthetic analysis for extracting information on soil salinity using remote sensing and GIS: A case study of Yamggao Basin, China. *Environmental Management*, **22**, 153–159.

Pierson, D. C., 1998, Measurement and modeling of radiance reflectance in Swedish water. In *Proceedings of 1st EARSeL Workshop on Imaging Spectroscopy, Zurich, Switzerland 6–8 October 1998* (Paris: EARSEL), pp. 207–214.

Richter, R., 1996, Atmospheric correction of DAIS hyperspectral image data. *Computers and Geophysics*, **22**, 785–793.

Richter, R., and Ludeker, W., 1998 Retrieval of atmopsheric water vapour from MOS-B imagery. In *Proceedings of 1st EARSeL Workshop on Imaging Spectroscopy, Zurich, Switzerland 6–8 October 1998* (Paris: EARSEL), pp. 201–206.

Roberts, D. A., Yamaguchi, Y., and Lyon, R. J. P., 1985 Calibration of airborne imaging spectrometer data to percent reflectance using air born imaging spectrometer data to percent reflectance using field spectral measurements. In *Proceedings of the Nineteenth International Symposium on Remote Sensing of the Environment. Ann Arbor, Michigan, 21–25 October 1985* (Ann Arbor: ERIM), pp. 21–25.

Stark, E., Luchter, K., and Margoshes, M., 1986, Near-infrared analysis (NIRA): A technology for quantitative and qualitative analysis. *Applied Spectroscopy Reviews*, **24**, 335–339.

Stoner, E. R., and Baumgardner, M. F., 1981, Characteristic variation in reflectance of surface soils. *Soil Science Society of American Journal*, **45**, 1161–1165.

Udelhoven, T., Hill, J., Imeson, A., and Cammeraat, H., 1997, A neural network approach for the identification of the organic carbon content of soils in a degraded semiarid ecosystem (Guadalentin, SE, Spain) based on hyperspectral data from the DAIS-7915 sensor. In *Proceedings of 1st EARSeL Workshop on Imaging Spectroscopy, Zurich, Switzerland 6–8 October 1998* (Paris: EARSEL), pp. 437–444.

Vane, G., Green, R. O., Chrien, T. G., Enmark, H. T., Hansen, E. G., and Porter, W, M., 1993, The airborne visible/infrared imaging spectrometer (AVIRIS). *Remote Sensing of Environment*, **44**, 127–143.

Zhang, L., Li, D., Tomg, Q., and Zheng, L., 1998, Study of the spectral lake area, China. *International Journal of Remote Sensing*, **19**, 2077–2084.